Journal of Biomechanics 43 (2010) 714–719

Contents lists available at ScienceDirect

Journal of Biomechanics

journal homepage: www.elsevier.com/locate/jbiomech
www.JBiomech.com

Failure mechanism of the all-polyethylene glenoid implant

Junaid Sarah [a], Gupta Sanjay [a], Sanghavi Sanjay [a], Anglin Carolyn [b], Roger Emery [c,d], Amis Andrew [a,c], Hansen Ulrich [a,*]

[a] Department of Mechanical Engineering, Imperial College London, Exhibition Road, London, SW7 2AZ, UK
[b] Centre for Bioengineering Research & Education and Department of Civil Engineering, University of Calgary, Canada, T2 N 1N4
[c] Musculoskeletal Surgery, Imperial College London, London, W6 8RF, UK
[d] Department of Orthopaedic Surgery, St. Mary's Hospital, London, UK

ARTICLE INFO

Article history:
Accepted 5 October 2009

Keywords:
Glenoid
Loosening
Fixation failure

ABSTRACT

Fixation failure of glenoid components is the main cause of unsuccessful total shoulder arthroplasties. The characteristics of these failures are still not well understood, hence, attempts at improving the implant fixation are somewhat blind and the failure rate remains high. This lack of understanding is largely due to the fundamental problem that direct observations of failure are impossible as the fixation is inherently embedded within the bone.

Twenty custom made implants, reflecting various common fixation designs, and a specimen set-up was prepared to enable direct observation of failure when the specimens were exposed to cyclic superior loads during laboratory experiments. Finite element analyses of the laboratory tests were also carried out to explain the observed failure scenarios.

All implants, irrespective of the particular fixation design, failed at the implant–cement interface and failure initiated at the inferior part of the component fixation. Finite element analyses indicated that this failure scenario was caused by a weak and brittle implant–cement interface and tensile stresses in the inferior region possibly worsened by a stress raiser effect at the inferior rim.

The results of this study indicate that glenoid failure can be delayed or prevented by improving the implant/cement interface strength. Also any design features that reduce the geometrical stress raiser and the inferior tensile stresses in general should delay implant loosening.

1. Introduction

Glenoid loosening constitutes 32% of all total shoulder arthroplasty (TSA) complications and has a revision rate of 7% (Bohsali et al., 2006). To overcome this, curved-back designs, variations in pegged or keeled designs and other macro-features have been used. Despite many efforts, the optimal design parameters are still not established. This difficulty is probably caused by the fact that, fundamentally, the characteristics of failure are not yet clear.

Previous studies have indicated failure to occur; around the the keel/pegs (Klepps et al., 2005; Trail and Nuttall, 2002); in the superior region (Nagels et al., 2002) or in the inferior region (Nagels et al., 2002). Most clinical studies report failure to occur in the cement/bone interface (Yian et al., 2005). However, most of these studies base their findings on the presence of radiolucent lines, which, apart from being difficult to quantify and understand the significance of, are also unlikely to capture narrow de-bonds at the implant/cement interface or thin cracks in the bulk cement. Therefore, the findings from these radiographic studies are questionable and there are retrieval studies that show results indicating failure to occur wholly (Nyffeler et al., 2003) or partly (Yian et al., 2005) in the implant/cement interface. Finally, some studies describe failure of the bulk cement (Terrier et al., 2005). In summary, the location of failure along and within the fixation is not well established.

It is the purpose of this paper to determine characteristics such as: (1) does the failure initiate inferiorly, superiorly or at the keel/pegs? (2) What is the weakest link in the fixation; the cement, the bone or at the interfaces? Knowing which of the constituents that is the weakest link will determine if, for example, stronger cement would be beneficial or if more optimal surface preparation techniques are required to improve glenoid fixation.

Based on the concept of the "rocking horse effect" (Matsen et al., 1994) and the work by Anglin, 1999, the American Society for Testing and Materials (ASTM) adopted a standard for testing of glenoid implant loosening (ASTM F 2028-02, 2004). This method uses a measure of changing implant rim displacement with number of load cycles as an indicator of loosening. However, the measure of rim displacement is only an indirect measure of fixation

* Corresponding author. Tel.: +44 207 594 7061; fax : +44 207 581 5495.
E-mail address: u.hansen@ic.ac.uk (H. Ulrich).

0021-9290/$ - see front matter © 2009 Elsevier Ltd. All rights reserved.
doi:10.1016/j.jbiomech.2009.10.019

failure and it has not, in fact, been shown that an increase in rim displacement correlates with initial or progressive loosening.

The reason for using these questionable, indirect measures is that the fixation is inherently embedded in the bone and impossible to observe directly. To overcome this problem, custom made implants (see Fig. 1) allowing direct observation of the fixation and the progressive failure were used in this study. These specimens are clearly different from real implants but the simple justification is that, whatever the shortcomings, it is the only way to be able to observe failure directly. Also, as will be discussed later, a recent study (Gregory et al., 2009) using real implants supports the use of these specimens.

2. Materials and Methods

2.1. Mechanical test

Modified glenoid specimens were manufactured and will be referred to as two-dimensional or 2D specimens in this paper. The cross-sectional dimensions in the coronal plane of commercially available keeled and pegged glenoids were extruded by 40 mm normal to the coronal plane to create 2D implants (Fig. 1). A testing rig in compliance with the ASTM standard (ASTM F 2028-02, 2004) was used to carry out the cyclic testing (Fig. 2). The glenoid specimens articulated against a humeral head. The humeral head was a semi-circular cylinder, 24 mm radius by 40 mm long, corresponding to the 2D geometry of the glenoid components (Fig. 2). The glenoid implants were CNC machined from ultra high molecular weight polyethylene or UHMWPE (RS catalogue, 2004). In total, twenty implants of different design parameters were manufactured to make a total of 8 specimen groups (Table 2); peg versus keel, flat-back versus curve-back, conforming (25 mm glenoid radius) versus less conforming (29 mm glenoid radius).

The implants were cemented into porous polyurethane (PU) bone substitute, which has properties (see Table 1) representative of the rheumatoid bone (Yang et al., 1997) present in many TSA cases. The PU parts were also CNC machined and designed to accommodate a uniform 2 mm thick cement mantle (Couteau et al., 2001). Stryker Simplex® polymethylmethacrylate (PMMA) bone cement was hand mixed at room temperature and introduced using finger pressure and a cement layer on both the bone and implant side. The implantation was carried out by an experienced shoulder surgeon (S.S.).

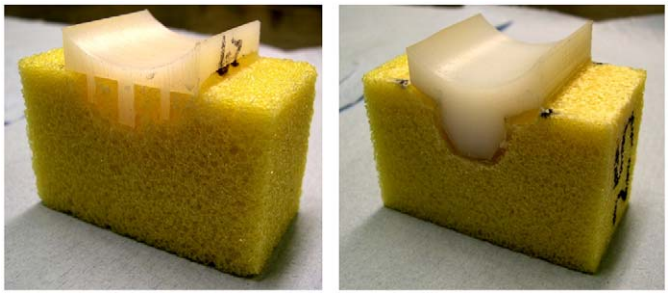

Fig. 1. Cemented 2D-specimen in bone substitute; flat-back peg (left) and curved-back keel (right).

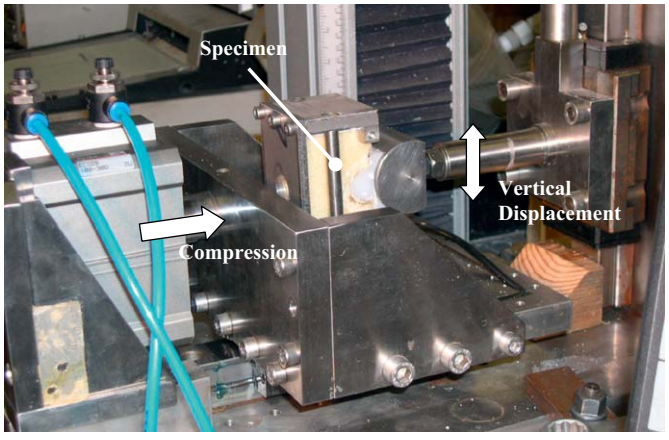

Fig. 2. The ASTM F2028-08 biaxial testing rig, modified according to the 2D configuration of this study.

Table 1
Material properties used in the FE model.

Material	Young's Modulus, GPa	Poisson's Ratio
UHMWPE implant[a]	0.6	0.4
PMMA bone cement[b]	2.2	0.3
PU bone substitute[c]	0.0475	0.3

[a] White polyethylene rod from manufacturer's data sheet (RS, 2004).
[b] (Lewis et al., 1997).
[c] Cellular rigid polyurethane foam 12.5 pcf (Sawbones product catalogue, 2009).

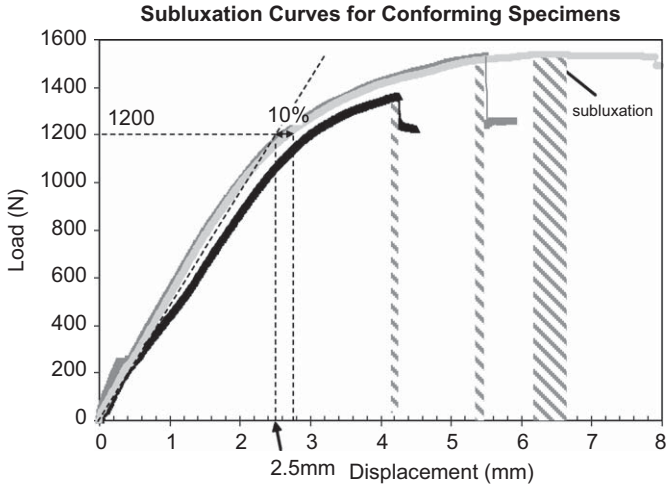

Fig. 3. Subluxation curve of three conforming specimens with loading point derived at the linear section of the curve (dotted). Note: displacement range (shaded) at point of subluxation.

The humeral head was compressed into the glenoid using a horizontal load of 1800 N applied by a pneumatic cylinder. This load is higher than the compressive load specified in the ASTM standard but is not physiologically unreasonable (Anglin et al., 2000a). The 2D implants were bulkier and stiffer structures than real implants, so higher loads were applied in order to generate stresses in the 2D fixation that were similar to the stresses in the fixation of a real implant (as determined from a finite element model of the two cases).

In addition to the constant horizontal load applied through the glenoid, the specimens were loaded by displacing the humeral head vertically at 0.5 Hz in sets of 4000 cycles via displacement control. The humeral head was displaced superiorly (that is, vertically upwards) from the centre of the glenoid and back to the centre. This imposed compressive stresses mostly onto the superior part of the fixation and tensile stresses mostly on the inferior part of the glenoid fixation, thereby making it easier to understand the type of failure observed. This loading regime does not seem unreasonable as, clinically, superior migration and loads are more common (Bergmann et al., 2007; Trail and Nuttall, 2002).

Prior to fixation failure testing, two specimens of each design were tested qausi-statically to determine the load and displacement to subluxation. The ASTM standard specifies that 90% of the subluxation displacement must be determined and used as the vertical displacement during the cyclic test. However, it was not easy to determine the 90% subluxation displacement. This was due to: (1) the force–displacement response being very flat near the subluxation point (Fig. 3) making it difficult to accurately determine the subluxation displacement; (2) great inter-specimen variability of the non-linear behaviour in the near-subluxation region (Fig. 3), resulting in significant scatter of the 90% subluxation displacement between specimens. Instead, the load and displacement at the end of the linear region of the curve, where there was much less variability between specimens, were used (Fig. 3). The end of the linear region was defined as the point when there was a 10% displacement difference between the (average) non-linear response and an extrapolation of the linear region (Fig. 3). This approach led to 2.5 mm for the conforming designs and 3.25 mm for the less conforming designs

or 1200 and 1100 N, respectively. That is, approximately 83% of the average subluxation load. Although these loads were slightly lower than would have been the result of strictly applying the 90% ASTM recommendation, they were still near-subluxation loads, which is the principal recommendation of the ASTM standard.

2.2. FE analysis

To represent each of the implant configurations, eight 2D models were built using between 8800 and 14,400 quadrilateral elements. The materials were modelled as linear elastic and the relevant properties are shown in Table 1. The FE analysis was carried out in Marc/Mentat 2005 (MSC Software, Palo Alto, CA) and modelled as a plane strain problem. The humeral head was assumed rigid with a friction coefficient of 0.07 between the humeral head and glenoid implant (Anglin et al., 2000b). The interfaces between the UHMWPE and PMMA and the between PMMA and bone substitute, were modelled as fully bonded. The loading and boundary conditions mimicked the laboratory test set-up. Mesh convergence was verified.

Predicted stresses, normal and tangential to the interfaces, were used to evaluate the risk of failure of the implant/cement and cement/bone interfaces. The maximum principal stress was used to evaluate the risk of failure of the cement mantle. The minimum principal stresses were used to predict bone crushing.

To predict failure the stresses were compared to relevant strength values. Unpublished work in our laboratory has found the cement/bone-substitute interface tensile strength to be *greater* than 2.32 ± 0.54 MPa. The strength of the polyethylene-implant/PMMA bone cement interface depends on the roughness of the polyethylene surface. Unpublished work in our laboratory has found the tensile strength of this interface to range between virtually zero and 3.2 MPa for realistic implant surface roughness (that is, roughness ranging from "smooth" to 5.5 μm). The roughness of the backside of the polyethylene glenoids in this study was to 3–6 μm and it was assumed that the implant/cement interface strength for this study was in the range of 1 to 3.2 MPa. The tensile strength of PMMA bone cement is 27.1 MPa (Krause and Hofmann, 1989) and the compressive strength of the bone substitute is 3.9 MPa (Sawbones product catalogue, 2009).

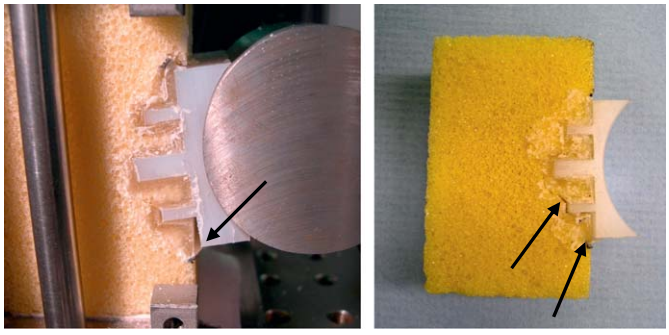

Fig. 4. In all cases failure (indicated by arrows) was observed in the implant/cement interface and initiated in the inferior part of the fixation. In the figure, inferior is the lower part of the fixation and superior is the upper part of the fixation.

3. Results

3.1. Cyclic testing

In all twenty specimens, irrespective of design type, failure was observed at the implant/cement interface (Fig. 4). Initial failure occurred at the inferior edge of the glenoid component and propagated superiorly across the back of the glenoid until it met a fixation feature. The crack propagated around the periphery of the fixation keels. However, for pegged designs, the crack propagated as far as the tip of the inferior peg and then 'jumped' across the bone to the tip of the next peg where failure progressed at the cement/bone interface (Figs. 4 and 5). Progressive superior bone crushing was also observed. Cycles to failure varied between 8000 and 14,905 cycles (Table 2), failure being defined as the crack having reached the centre line of the implant (Fig. 5). The number of cycles to failure shown in Table 2 can be used to compare the different implant designs but the results of this 2D study should not be used to quantitatively estimate real life time survival.

3.2. FE results

Fig. 6 shows the predicted stresses in the fixation of the curved-back, keeled implant. While there were differences in stresses between the different implant designs, this figure demonstrates the characteristic features of the stress distributions for all the implants and is used to demonstrate the FE results. The figure also includes the strength values, mentioned earlier, of the various components of the fixation.

The normal stress along the implant/cement interface was predominantly compressive superiorly and tensile inferiorly. The average tensile stress in the inferior region was 0.83 MPa and

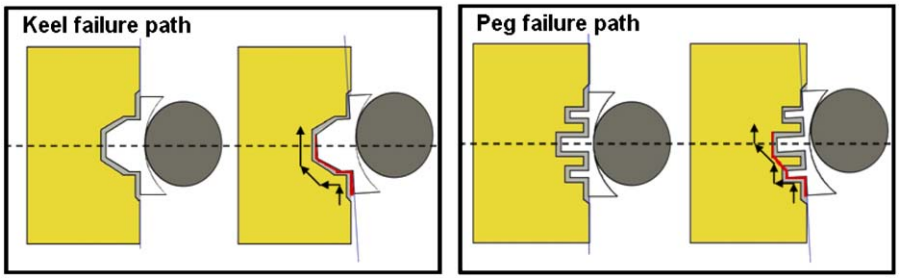

Fig. 5. Failure pathway in keeled (left) and pegged glenoids (right). A similar failure path was observed for all design configurations. In the figure, inferior is the lower part of the fixation and superior is the upper part of the fixation.

Table 2
Results showing average, and in brackets the standard deviation, number of cycles to failure for different implant designs. Number of samples is '*n*'.

	 Flat-back peg	 Flat-back keel	 Curve-back keel	 Curve-back peg
Less conforming (5 mm radial mismatch)	8275 (7 0 6), *n*=4	9764 (5 2 5), *n*=4	10,519 (8 5 8), *n*=4	13,150 (7 6 3), *n*=4
Conforming (1 mm radial mismatch)	13,969, *n*=1	12,297, *n*=1	14,905, *n*=1	12,100, *n*=1

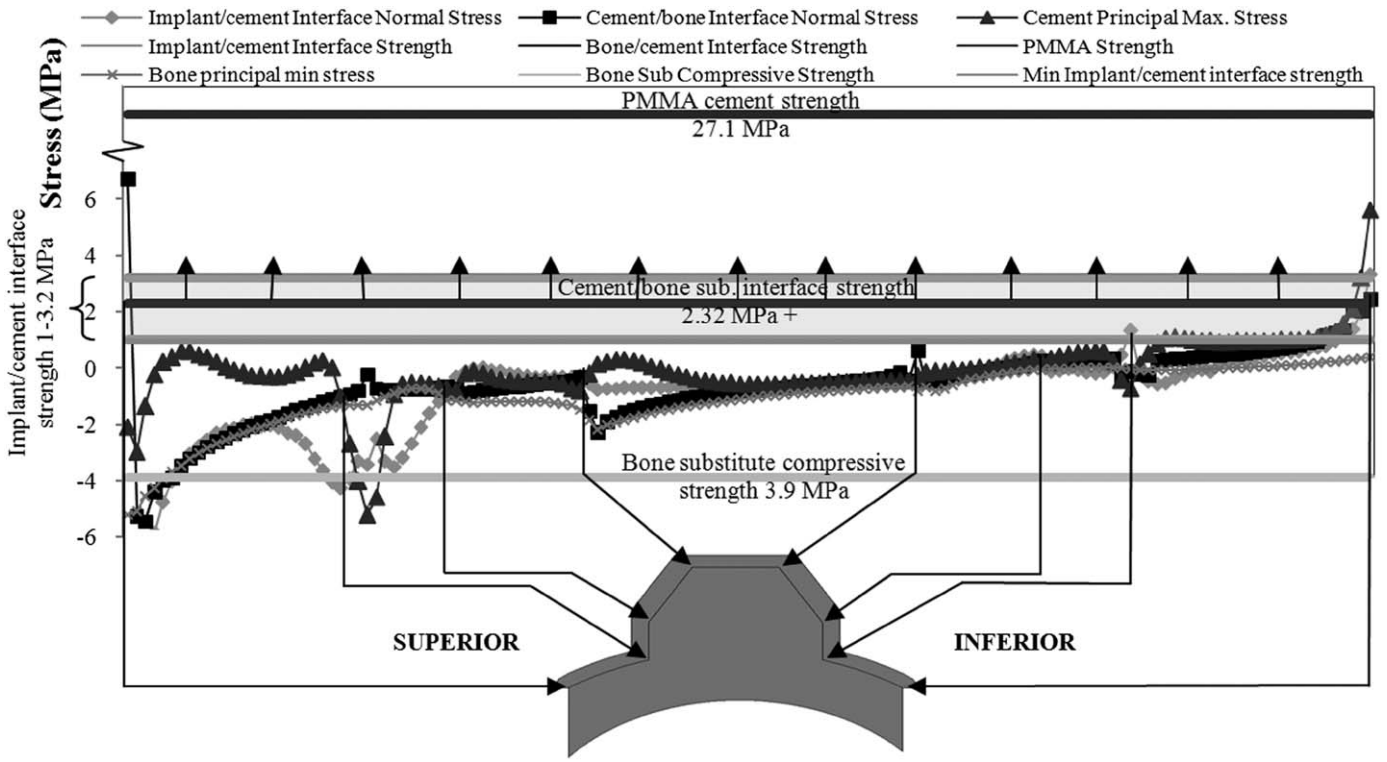

Fig. 6. Plot of the predicted stresses in the fixation of the curve-back keel specimen. The plotted stresses are at: the two interfaces; in the bulk PMMA bone cement and in PU bone substitute. The strengths of the two interfaces, of the cement and of the PU bone substitute are also shown. The implant/cement interface strength is only known within a range and this range is indicted by the hatched area. Only a minimum value of the cement/bone-substitute strength is known (2.32 MPa) and the arrows indicate that the strength is likely to be higher than 2.32 MPa.

increased to 3.35 MPa towards the edge and were within the range of the implant/cement interface strength of 1–3.2 MPa, indicating that failure of this interface is likely. In contrast, the maximum principal stresses in the cement were much lower than the tensile strength of the PMMA bone cement (27.1 MPa). The stresses in the cement/bone interface were also tensile in the inferior zone and reached the cement/bone interface strength, conservatively estimated to be 2.32 MPa, only in the small region very close to the edge.

The minimum principal (compressive) stresses in the underlying bone substitute in the superior part of the fixation are predicted to reach −5.2 MPa, exceeding the 3.9 MPa compressive strength of the PU bone substitute. This predicted bone substitute crushing in the superior region was also observed during the experiments (Fig. 4).

4. Discussion

All implants, irrespective of the particular fixation design, failed at the implant–cement interface and failure initiated at the inferior edge part of the component fixation. Finite element analyses indicated that this failure scenario was caused by a weak implant/cement interface strength and relatively high tensile stresses in the inferior region, possibly worsened by a stress concentration at the inferior edge, where tensile stresses are highest. Crushing of the bone substitute in the superior region was also apparent.

4.1. Location of failure

Clinical radiographic studies have found radiolucent lines around the peg/keel which have been interpreted as a loss of fixation (Barrett et al., 1987; Hertel and Ballmer, 2003). Other studies (Nagels et al., 2002; Nuttall et al., 2007; Yian et al., 2005) have reported radiolucent lines inferiorly. In particular, Nagels et al. (2002) found that radiolucent lines grew over time inferiorly, while radiolucent lines existed in the superior part of the fixation immediately following the surgery (Nagels et al., 2002), possibly indicating the critical nature of inferior radiolucent lines.

Failure of the fixation in the inferior region was the obvious failure mode in all specimens, which is consistent with the clinical studies just mentioned. The finite element analysis showed that this region is exposed to tensile stresses and interfaces are typically weak in tension. The tensile stresses increased rapidly towards the inferior edge (Fig. 6), due to the geometry of the edge of the component. Although the edge of the 2D set-up may not have represented the real implant features accurately, the analysis does demonstrate that implant failure may be sensitive to subtle details of the edge geometry, which could probably be modified to lower the risk of failure.

4.2. The weakest link of the fixation

PMMA bone cement has been a cause for concern in implant loosening because it is known to be weak in tensile fatigue (Saha and Pal, 1984). It is often presumed that the cement is the weakest link in the fixation (Hopkins et al., 2004; Lacroix and

Prendergast, 1997). However, in this study there were no indications that cement was fracturing and the cement stresses were predicted to be very much lower than both the tensile strength of cement of 27.1 MPa and the fatigue strength of 10 MPa (Murphy and Prendergast, 2000). Thus, the bulk cement is unlikely to be the weakest part of the fixation.

In this study, the bone substitute was crushed superiorly and finite element predictions also found stresses indicative of compressive failure. This may explain the radiolucent lines observed in clinical studies. However, this interpretation has to be viewed in the context that this study used bone substitute material, which may have a lower compressive strength (3.9 MPa) than real glenoid bone (10.3 MPa, Anglin, 1999). However, rheumatoid bone strength is likely to be much lower (Yang et al., 1997) and possibly reasonably represented by the bone substitute strength. Also the compressive stresses in the superior region of the 2D set-up are possibly larger than in the physiological (3-dimensional) implant fixation.

An important limitation of this study is the use of the possibly non-physiological 2D set-up. The simple justification for the 2D set-up is that, whatever its shortcomings, it is the only way to be able to observe failure directly. A recent study, that was in many ways similar to the present study but using real (3D) implants, also found that failure took place at the implant/cement interface (Gregory et al., 2009). It would therefore seem that the 2D set-up is reasonably representative of physiological conditions.

Another limitation related to the 2D nature of the study is that no grooves or other macrofeatures at the glenoid back were included. The effects of such macrofeatures will undoubtedly depend on their specific geometry but is unlikely to change the recommendation of this study to increase the PE–cement interface strength. Similarly, real implants usually contain notches or holes in the polyethylene keel or pegs to create an interlock to help prevent the implant from simply slipping out of the cement. These features would possibly delay failure but, as mentioned above, the study by Gregory et al. (2009), indicated that it would not change the recommendation to increase the PE–cement interface strength.

The stresses predicted for the implant/cement interface were of similar magnitude to those at the bone-substitute/cement interface. Possibly it could be argued that the strength of the bone-substitute/cement interface (*greater* than 2.32 MPa) is higher than the implant/cement interface strength (1–3.2 MPa) and that this would explain why it was consistently the implant/cement interface that was observed to fracture. Furthermore, the fracture of the implant/cement interface appeared brittle (there was no cement attached to the fracture surface of the polyethylene and no polyethylene attached to the fracture surface of the cement). It may be that the implant/cement interface is more brittle than the cement interdigitised bone-substitute/cement interface. Perhaps to fully explain the observed failure scenario a fracture mechanics approach is necessary.

Although using bone substitute material instead of real glenoid bone is a limitation of the study, unpublished work in our laboratory has shown that the glenoid-bone/cement interface strength is higher than the bone-substitute/cement interface strength. It would therefore seem unlikely that using the stronger glenoid bone would have changed the finding that the implant/cement interface is the weakest link.

The conditions of the implantation in this laboratory study were ideal. In the clinical situation factors such as poor cementing (including a non-uniform cement mantle), bone preparation techniques and the presence of interstitial fluids may lead to very much lower cement/bone interface strengths. Although surgical techniques are continuously being improved in order to minimise the effect of such factors they are still very real, and probably they do adversely affect clinical loosening (Norris and Lachiewicz, 1996). However, the scope of this study was not to investigate the effects of imperfect surgical techniques.

The results of this study contrast with the apparent consensus from clinical studies (primarily radiographic) that loosening is at the cement/bone interface (Bohsali et al., 2006; Matsen et al., 2008). However, radiolucent lines have been attributed to a formation of fibrous connective tissue (Wirth et al., 2001). It is unlikely that there would be any soft tissue at a debonded implant/cement interface. One possible reason that the clinical studies do not report implant/cement interface failures may be that such failures are not captured on radiographs, even when present. There are also retrieval studies that show clinical failure to take place wholly (Nyffeler et al., 2003) or partly (Yian et al., 2005) at the implant/cement interface. It may also be that the failure scenario cannot be explained completely as taking place at just one interface. The results shown for the pegged implant in Figs. 4 and 5 show such a mixed failure scenario where fixation fracture initiates in the implant/cement interface but later propagates through the cement and into the bone and bone–cement interface.

Some authors have suggested that glenoid failure is due to a biological reaction caused by polyethylene wear particles (Wirth et al., 1999). Such biological reactions at the cement–bone interface cannot be accounted for in our in-vitro study and could also explain why cement/bone interface failure is not observed in this study. Even if this is the case, the results of this study may still be clinically relevant in a similar manner to the clinical relevance of in-vitro studies of, for example, poor cementing or bone preparation techniques. Such factors may be most directly relevant to early loosening or to early stages of clinical (gross) loosening. Early stages of fixation failure are difficult to observe in clinic and may differ from the later stage failures that can be observed clinically. However, any such factor that may influence early fixation failure, may in turn have an effect on long-term failures that may or may not be influenced by biological reactions.

5. Conclusions

A 2D laboratory set-up enabled, for the first time, direct observations of glenoid fixation failure, which was shown to initiate in the inferior part of the fixation, the implant/cement interface being the weakest part of the fixation. The results indicated that efforts to strengthen PMMA bone cement are unlikely to have any effect on glenoid loosening because the cement is not the weakest link.

The results indicated that strengthening the polyethylene implant/cement interface, for example by roughening the polyethylene surface, will improve the fixation strength of glenoid implants. Also, design features that lead to overall lower tensile stresses inferiorly and in particular features that reduce the stress raiser at the edges of the fixation are likely to improve implant loosening performance.

While strengthening the polyethylene implant/cement interface can only be advantageous, the impact of the recommendations of this paper should be viewed in the context that clinically most failures are believed to occur at the bone/cement interface.

Conflict of interest

The authors declare that there is no conflict of interest that could inappropriately influence the results of the current research work.

Acknowledgements

The authors would like to acknowledge Arthritic Research Campaigns (ARC) for funding the work in this study.

References

Anglin, C., 1999, Shoulder Prosthesis Testing. Ph.D. Thesis, Queen's University Press, Ontario.

Anglin, C., Wyss, U.P., Pichora, D.R., 2000a. Arm motion and load analysis of sit-to-stand, stand-to-sit, cane walking and lifting. Clinical Biomechanics 15 (6), 441–448.

Anglin, C., Wyss, U.P., Pichora, D.R., 2000b. Mechanical testing of shoulder prostheses and recommendations for glenoid design. Journal of Shoulder and Elbow Surgery 9 (4), 323–331.

ASTM F 2028-02, 2004. Standard test methods for the dynamic evaluation of glenoid loosening or disassociation. Book of ASTM Standards, 1083–1088.

Barrett, W.P., Franklin, J.L.E.J.S., Wyss, C.P., Matsen, F.A., 1987. Total Shoulder Arthroplasty. Journal of Bone and Joint Surgery 69A (6), 865–872.

Bergmann, G., Graichen, F., Bender, A., Kaab, M., Rohlmann, A., Westerhoff, P., 2007. In vivo glenohumeral contact forces-Measurements in the first patient 7 months postoperatively. Journal of Biomechanics 40, 2139–2149.

Bohsali, K.I., Wirth, M., Rockwood, C.A., 2006. Complications of total shoulder arthroplasty. Journal of Bone and Joint Surgery American Volume 88 (10), 2279–2292.

Couteau, B., Mansat, P., Estivalezes, E., Darmana, R., Mansat, M., Egan, J., 2001. Finite element analysis of the mechanical behaviour of a scapula implanted with a glenoid prosthesis. Clinical Biomechanics 16, 566–575.

Gregory, T., Hansen, U., Taillieu, F., Baring, T., Brassart, N., Mutchler, C., Amis, A.A., Augereau, B., Emery, R., 2009. Glenoid loosening after total shoulder arthroplasty: and in-vitro CT-scan study. Journal of Orthopaedic Research (accepted).

Hertel, R., Ballmer, F.T., 2003. Observations on retrieved glenoid components. The Journal of Arthroplasty 18 (3), 361–366.

Hopkins, A.R., Hansen, U., Amis, A., Emery, R., 2004. The effects of glenoid component alignment variations on cement mantle stresses in total shoulder arthroplasty. Journal of Shoulder and Elbow Surgery 13 (6), 668–675.

Klepps, S., Chiang, A.S., Miller, S., Jiang, C.Y., Hazrati, Y., Flatow, E.L., 2005. Incidence of early radiolucent glenoid lines in patients having total shoulder replacements. Clinical Orthopaedics and Related Research 435, 118–125.

Krause, W., Hofmann, A., 1989. Antibiotic impregnated acrylic bone cements: a comparative study of the mechanical properties. Journal of Bioactive and Compatible Polymers 4, 345–361.

Lacroix, D., Prendergast, P.J., 1997. Stress analysis of glenoid component designs for shoulder arthroplasty. Proceedings of the Institute of Mechanical Engineering Part H: Journal of Engineering in Medicine 211, 467–474.

Lewis, G., Nyman, J.S., Trieu, H.H., 1997. Effect of mixing method on selected properties of acrylic bone cement. Journal of Biomedical Materials Research 38 (3), 221–228.

Matsen, F.A., Clinton, J., Lynch, J., Bertelsen, A., Richardson, M.L., 2008. Glenoid component failure in total shoulder arthroplasty. The Journal of Bone and Joint Surgery 90A (4), 885–896.

Matsen, F.A., Lippitt, S.B., Sidles, J.A., Harryman, D.T., 1994. In: Practical Evaluation and Management of the Shoulder. Saunders, Philadelphia.

Murphy, B.P., Prendergast, P.J., 2000. On the magnitude and variability of the fatigue strength of acrylic bone cement. International Journal of Fatigue 22 (10), 855–864.

Nagels, J., Valstar, E.R., Stokdijk, M., Rozing, P.M., 2002. Patterns of loosening of the glenoid component. Journal of Bone and Joint Surgery 84B (1), 83–87.

Norris, B.L., Lachiewicz, F., 1996. Modern cement technique and the survivorship of total shoulder arthroplasty. Clinical Orthopaedics and Related Research 328, 76–85.

Nuttall, D., Haines, J.F., Trail, I.I., 2007. A study of the micromovement of pegged and keeled glenoid components compared using radiostereometric analysis. Journal of Shoulder and Elbow Surgery 16 (3), 65S–70S.

Nyffeler, R.W., Anglin, C., Sheikh, R., Gerber, C., 2003. Influence of peg design and cement mantle thickness on pull-out strength of glenoid component pegs. Journal of Bone and Joint Surgery 85B (5), 748–752.

RS catalogue, 2004. White polyethylene rod datasheet, RS Components Ltd., http://uk.rs-online.com.

Saha, S., Pal, S., 1984. Mechanical properties of bone–cement—a review. Journal of Biomedical Materials Research 18 (4), 435–462.

Sawbones product catalogue, 2009. Sawbones Europe AB a division of Pacific Research Laboratories, Inc., Malmö, Sweden.

Terrier, A., Buchler, P., Farron, A., 2005. Bone–cement interface of the glenoid component: stress analysis for varying cement thickness. Clinical Biomechanics 20 (7), 710–717.

Trail, I.A., Nuttall, D., 2002. The results of shoulder arthroplasty in patients with rheumatoid arthritis. Journal of Bone and Joint Surgery 84B (8), 1121–1125.

Wirth, M.A., Agrawal, C.M., Mabrey, J.D., Dean, D.D., Blanchard, C.R., Miller, M.A., Rockwood, C.A., 1999. Isolation and characterization of polyethylene wear debris associated with osteolysis following total shoulder arthroplasty. Journal of Bone and Joint Surgery 81A (1), 29–37.

Wirth, M.A., Korvick, D.L., Basamania, C.J., Toro, F., Aufdemorte, T.B., Rockwood, C.A., 2001. Radiologic, mechanical, and histologic evaluation of 2 glenoid prosthesis designs in a canine model. Journal of Shoulder and Elbow Surgery 10 (2), 140–148.

Yang, J.P., Bogoch, E.R., Woodside, T.D., Hearn, T.C., 1997. Stiffness if trabecular bone of the tibial plateau in patients with rheumatoid arthritis of the knee. The Journal of Arthroplasty 12 (7), 798–803.

Yian, E.H., Werner, C.M.L., Nyffeler, R.W., Pfirrmann, C.W., Ramappa, A., Sukthankar, A., Gerber, C., 2005. Radiographic and computed tomography analysis of cemented pegged polyethylene glenoid components in total shoulder replacement. Journal of Bone and Joint Surgery 87A (9), 1928–1936.